

Article

Thermal neutron Relative Biological Effectiveness factors for Boron Neutron Capture Therapy from *in vitro* irradiations

María Pedrosa-Rivera¹, Javier Praena¹, Ignacio Porras^{1,*}, Manuel P. Sabariego¹, Ulli Köster², Michael Haertlein^{2,3}, V. Trevor Forsyth^{2,3,4}, José C. Ramírez⁵, Clara Jover⁵, Daniel Jimena⁵, Juan L. Osorio⁵, Patricia Álvarez⁶, Carmen Ruiz-Ruiz^{6,*} and María J. Ruiz-Magaña⁶

¹ Departamento de Física Atómica, Molecular y Nuclear, Facultad de Ciencias, Universidad de Granada, 18071 Granada, Spain.

² Institut Laue-Langevin, 71 Avenue des Martyrs, 38042 Grenoble Cedex 9, France.

³ Partnership for Structural Biology (PSB), 38042 Grenoble Cedex 9, France.

⁴ Faculty of Natural Sciences, Keele University, Staffordshire ST5 5BG, U.K.

⁵ Servicio de Radiofísica y Protección Radiológica, Hospital Universitario Virgen de las Nieves, Avda. Fuerzas Armadas 2, 18014 Granada.

⁶ Departamento de Bioquímica y Biología Molecular III e Inmunología, Facultad de Medicina, Universidad de Granada, 18016 Granada, Spain.

* Correspondence: porras@ugr.es (I.P.), mcarmenr@ugr.es (C.R.)

Abstract: The experimental determination of the relative biological effectiveness of thermal neutron factors is fundamental in Boron Neutron Capture Therapy. Present values have been obtained using mixed beams consisting of both neutrons and photons of various energies. A common weighting factor has been used for both thermal and fast neutron doses, although such an approach has been questioned. At the nuclear reactor of the Institut Laue-Langevin a pure low-energy neutron beam has been used to determine thermal neutron relative biological effectiveness factors. Different tumor cell lines, corresponding to glioblastoma, melanoma, and head and neck squamous cell carcinoma, and non-tumor cell lines (lung fibroblast and embryonic kidney) have been irradiated using an experimental arrangement designed to minimise neutron-induced secondary gamma radiation. Additionally, the cells were irradiated with photons at a medical linear accelerator, providing reference data for comparison with that from neutron irradiation. Survival and proliferation were studied after irradiation, yielding the Relative Biological Effectiveness corresponding to the damage of thermal neutrons for the different tissue types.

Keywords: Boron Neutron Capture Therapy; Relative biological effectiveness; thermal neutrons.

1. Introduction

Boron Neutron Capture Therapy (BNCT) is currently undergoing a renaissance that may bring this therapy closer to the hospital practice [1]. This is occurring as result of data from new accelerator sources, in combination with promising results from previous clinical trials at research reactors [2]. One of the new sources (Kyoto, Japan) has already started clinical trials [3]. In addition to this, the translation of recent research results from different disciplines to the clinical treatment may improve the therapeutic capability of this approach in the near future.

One line of improvement is treatment planning. In a clinical study performed at Helsinki University Central Hospital [4], results from two cohorts of patients receiving a differently planned tumor volume (PTV) dosing showed clearly that a small increase in the dose may lead to a much improved therapeutic outcome. The dose in BNCT, and in particular the “photon-equivalent”,

“photon-isoeffective” or “biologically weighted” dose is a key problem because the dose that the organs at risk may tolerate is a limiting factor in treatment planning and therefore limits the PTV. Therefore, increasing the accuracy of the estimation of this dose can lead to an improvement of the clinical treatment. The biologically weighted dose is currently estimated using fixed relative biological effectiveness (RBE) factors for the different components of the dose: thermal neutrons, fast (including epithermal) neutrons, boron and gamma [5], although recently, more accurate formalisms such as the photon iso-effective dose [6] and intermediate models have been proposed [7]. In all of these models, either the RBE factors or the alpha and beta radiobiological coefficients are required for both the BNCT dose components and for reference photon irradiation. It is therefore desirable to determine independently the experimental response to neutrons in the three energetic groups considered for BNCT: thermal ($E_n < 0.5$ eV), epithermal ($0.5 \text{ eV} \leq E_n \leq 10$ keV) and fast ($E_n > 10$ keV). In particular, the data currently used have been obtained by irradiation in a mixed field containing fast and thermal neutrons as well as gamma rays, and the subtraction of the gamma component may lead to large uncertainties if its contribution is large. Also, the mixing of fast and thermal neutrons has occurred usually in the previous experiments, and a common RBE factor for both has been adopted, whilst there has been some evidence against this assumption [8]. A spectrum-dependence of the neutron effect would mean that the RBE of the fast neutron dose could depend on the particular facility being used, and might be very different at reactor or accelerator-based sources. On the other hand, the RBE of thermal neutrons does not depend on the energy spectrum because the biological effect is mostly due to the high-energy products of the $^{14}\text{N}(n,p)^{14}\text{C}$ reaction (625.87 keV). Thus, in practice, a low energy neutron spectrum does not affect the energy of these products. Therefore, the RBE of thermal neutrons is a key factor in BNCT because does not depend on the facility.

The aim of this work was to measure the biological response of different cell lines (tumor and normal tissues) under a pure low energy neutron beam, with almost no contamination of fast neutrons and gamma radiation, and compare it with the response of the same cell lines under a reference photon irradiation from a hospital LINAC. For both kinds of irradiations, dedicated setups were designed. Two different biological end points have been studied for the determination of the neutron response, but for the thermal neutron RBE calculations only the common one (clonogenic ability) has been chosen

2. Materials and Methods

2.1. Neutron irradiations

Neutron irradiations were carried out at the PF1B cold neutron beam line at the Institut Laue-Langevin (ILL) [9]. The arrangement developed for neutron irradiation of culture cells has been described elsewhere [10]. This cold beam (lower energy than thermal) is equivalent to a thermal neutron beam because the energy delivered in the neutron interactions does not depend on its kinetic energy, and as a result of the $1/v$ behavior (where v is the neutron velocity) of neutron capture in the cold / thermal energy range, the thermal equivalent flux can be used to characterize the beam [10]. Hence in the following we discuss “thermal dose” even if the neutron spectrum used was actually “cold”. On PF1B the epithermal neutron and gamma contributions are negligible as a result of the bent guide. The thermal equivalent neutron flux at the sample position, as measured by gold foil irradiation, was $1.75 \times 10^9 \text{ n}_{\text{thermal}}/(\text{cm}^2\text{s})$. Figure 1 shows how this low energy spectrum, without any fast neutron contribution, is ideal for studies of the thermal factor, in contrast to some other neutron beams used in BNCT.

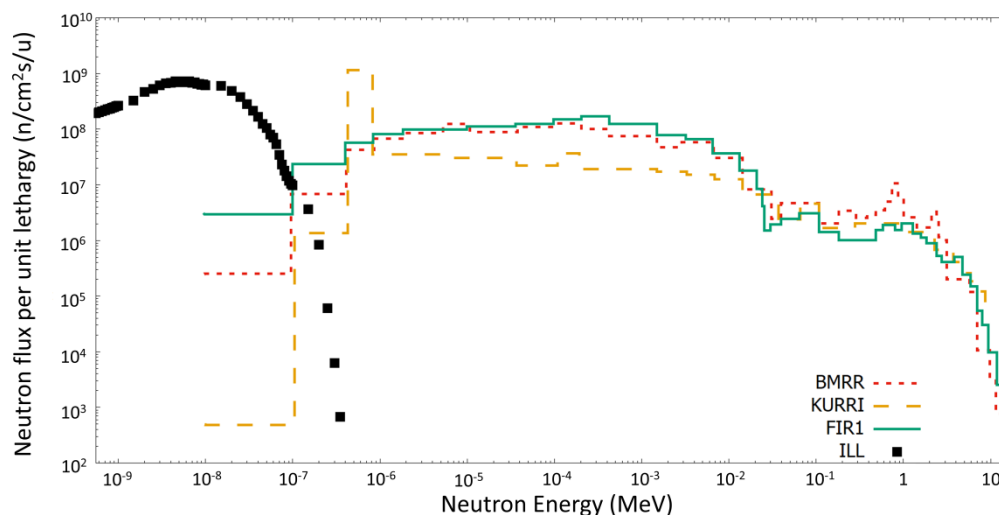


Figure 1. Simulated neutron spectrum at the end of the collimation system of the PF1B line at the Institut Laue-Langevin (ILL) (squares) when compared with epithermal neutron BNCT sources [11], such as the Brookhaven Medical Research Reactor (BMRR), Kyoto University Research Reactor Institute (KURRI) and Finland Reactor 1 (FIR1). Data is expressed in neutron flux per unit of lethargy.

The experimental arrangement shown in Figure 2 allowed two consecutive quartz cuvettes to be irradiated at the same time, with the second one receiving a lower dose than the first. In each cuvette the cells were attached to the cuvette surface perpendicular to the neutron beam. The gamma dose is due to the neutron capture with the quartz and the cell culture medium and stays lower than the neutron dose, making this instrument a very appropriate place to study the effect of low-energy neutrons. Cells were irradiated homogeneously during times ranging from 15 to 75 minutes.

2.2. Photons irradiations at medical linear accelerator

Photon irradiations were carried out at the medical linear accelerator (LINAC) of Virgen de las Nieves Hospital (HVN) in Granada. The Elekta Versa HD™ accelerator delivered a flattened 6 MV high energy photon beam [12]. The irradiation zone was adapted to carry out *in vitro* irradiations. The electronic equilibrium was secured by immersing the flasks in distilled water and placing under these 14 cm of solid water (see Figure 3). Two flasks are irradiated each time, both within the field of the beam, then receiving the same dose. Irradiations of 0.5-6 Gy were performed at 1 Gy/min dose rate.

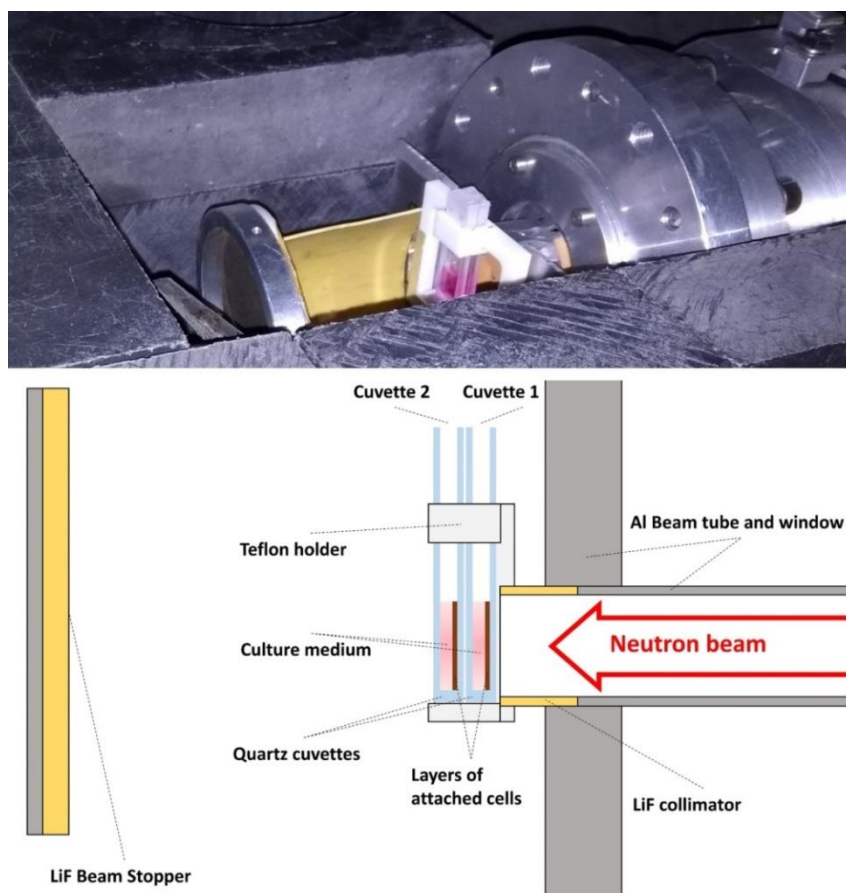


Figure 2. Picture and schematic cut view of the experimental arrangement installed on the PF1B instrument at the institute Laue-Langevin (ILL). Two cuvettes containing cells were irradiated at the same time. All the cells are irradiated homogeneously and the second cuvette receives a smaller dose than the first one. LiF is used as the first layer of collimators and as a beam stop, capturing neutrons without the generation of secondary gamma radiation.

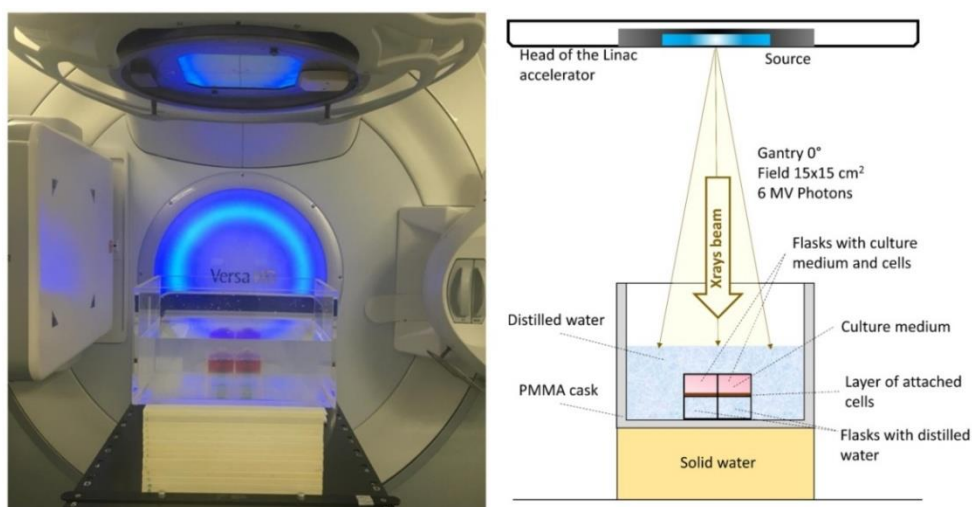


Figure 3. Experimental arrangements for cell irradiations with photons used at the medical linear accelerator in Granada. Two flasks with a layer of cells are irradiated at the same time with the same dose.

2.3. Dose estimation

Measurements of neutron flux were performed using gold foil activation data. Neutron doses at the cells were estimated with the MCNPx simulation code for the transport of the neutrons and the generated photons [13]. The geometry of the experimental arrangement was simulated accurately, calculating the dose by means of the kerma factor that depends on the nitrogen content of each cell line.

Photon doses at HVN medical LINAC were known from a computed tomography scan image and the clinically used treatment planning program (Pinnacle, Philips)[14].

2.4. Nitrogen content analysis

At thermal energies the neutron capture on nitrogen dominates the local dose deposition among all possible reactions in the tissue. The nitrogen content of the cells is therefore essential for the dose estimation. CHNS elemental analysis was performed with a THERMO SCIENTIFIC Flash 2000 (Thermo Fisher, Waltham, MA, USA) analyzer. CHNS elemental analyzers provide a means for the rapid determination of carbon, hydrogen, nitrogen and sulphur in organic matrices and other types of materials. It is based on the dynamic combustion of a sample. Resultant gases are separated and detected by a thermal conductivity detector (TCD). This technique can determine the quantity of carbon, nitrogen, hydrogen and sulphur with an error less than 3%.

Nitrogen content of HEK293 cells was measured by this method at the Centro de Instrumentación Científica (CIC) from the University of Granada.

2.5. Cells and cell culture

The six irradiated cell lines were of human origin, four from tumor tissue and two from healthy tissue. A375 cells are from malignant melanoma; Cal33 and SQ20 from head and neck squamous cell carcinoma; U87 from glioblastoma; HEK293 are from embryonic kidney; and MRC5 are fibroblast from fetal lung tissue. Cell lines were kindly provided from Institute of Advanced Biosciences, Grenoble, except for HEK293, which was acquired commercially (Thermo Fisher). The selected tumor cell lines correspond to the type of tumors that have been typically treated with BNCT. All of them are adherent cells, which is also a requirement in our set-up.

Cells were cultured in DMEM medium (HyClone, Logan, UT, USA) containing 10% fetal bovine serum (FBS; Gibco, Carlsbad, CA, USA), 1 μ M L-glutamine (Gibco), 100 IU/ml penicillin and 100 IU/ml streptomycin (Sigma-Aldrich, St. Louis, MO, USA) at 37°C in a humidified CO₂ 95% air incubator.

For irradiations, cells were cultured at 70% confluence in either quartz cuvettes (for neutron irradiation) or T25 flasks (for photon irradiation).

2.6. Clonogenic assays

Irradiated cells were detached with 1% trypsin-EDTA (Sigma-Aldrich) and prepared for clonogenic assays. Cells were seeded at appropriate dilutions, based on the irradiation dose and the growing characteristics of the cell line, to form colonies in around two weeks. Colonies were fixed with 90% ethanol, stained with crystal violet and counted using the open access automatic counter program by Nghia Ho [15].

2.7. Proliferation assays

After irradiation, cells were cultured in 96-well plates and incubated for four days. Proliferative ability was determined by a 5-bromo-2-deoxyuridine (BrdU) ELISA kit (Roche, Mannheim, Germany), following the manufacturer's instruction.

3. Results

3.1. Dosimetry

For ILL neutron irradiation studies, with nitrogen concentration in the cell lines ranging from 1.7 to 5.6%, simulated neutron thermal doses rates varied from 0.017 to 0.059 Gy/min, depending on the tissue type. For HEK293 cells, the nitrogen content measured with the elemental analyzer is in good agreement with the reference in ICRU report 46 for fetus kidney [16]. The nitrogen content for the remaining cell lines are those corresponding to their similar tissues from the references indicated in Table 1. For Cal33 and SQ20, the nitrogen content of squamous cell carcinoma was not found in literature so the default content of an average tissue, called ICRU-33, was selected [16]. It should be noted that the thermal dose is nearly entirely ($\approx 97\%$ contribution) due to neutron captures on nitrogen [17]. Hence a variation in nitrogen concentration leads in first order to a proportional change of thermal dose. Both, the assumed nitrogen content and the resulting thermal dose, are shown in Table 1. Thus, should new measurements of nitrogen content in certain cell lines become available, one could easily rescale this dose, the resulting α and β values in table 2 and the RBE in table 3.

Gamma doses, mainly from neutron interaction with the experimental system, are tissue-independent and therefore are the same for all cell lines. In all the cases, the thermal dose component remained higher than the gamma dose component (see Table 1). The main objective of the irradiations, which was to have a dose mostly due to low-energy neutrons, was achieved.

Table 1. Nitrogen content and dose components of the cell lines irradiated using the PF1B neutron beam instrument at the Institut Laue-Langevin (ILL). Campaign of June 2018.

Cell line	Nitrogen content (%)	Thermal dose, D_n (Gy/min)		Gamma dose, D_γ (Gy/min)	
		Cuvette 1	Cuvette 2	Cuvette 1	Cuvette 2
A375	5.6 [18]	0.059	0.028	0.013	0.010
Cal33	2.6 ¹	0.027	0.013	0.013	0.010
U87	2.2 [16]	0.023	0.011	0.013	0.010
SQ20	2.6 ¹	0.027	0.013	0.013	0.010
HEK293	1.7	0.017	0.008	0.013	0.010
MRC5	3.1 [16]	0.033	0.015	0.013	0.010

¹ value for average tissue ICRU-33 [16] used.

3.2. Results for neutron irradiation

Two end-points were studied for the neutron irradiations: survival, by means of clonogenic assay, and proliferation, by using BrdU incorporation assay, around two weeks and 4 days, respectively, after the irradiation. Plates for the visual appearance of these assays with A375 cells can be seen in Figure 4.

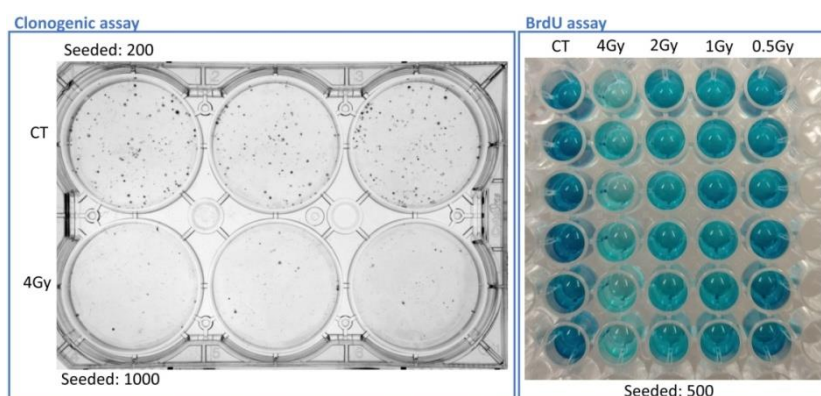


Figure 4. A375 plates for both clonogenic and proliferative assays. Left, plate for clonogenic assay with the control sample (CT) and the sample irradiated with a neutron dose of 4 Gy at day 7 after irradiation. Right, BrdU cell proliferation assay of control and irradiated cells at day 4 after irradiation. Samples were analyzed in triplicate for each data point.

As shown in figure 5, both end-points showed different results when data were fitted following a linear quadratic equation. The biggest difference between the survival and proliferation curves was observed in the head and neck tumor cell lines.

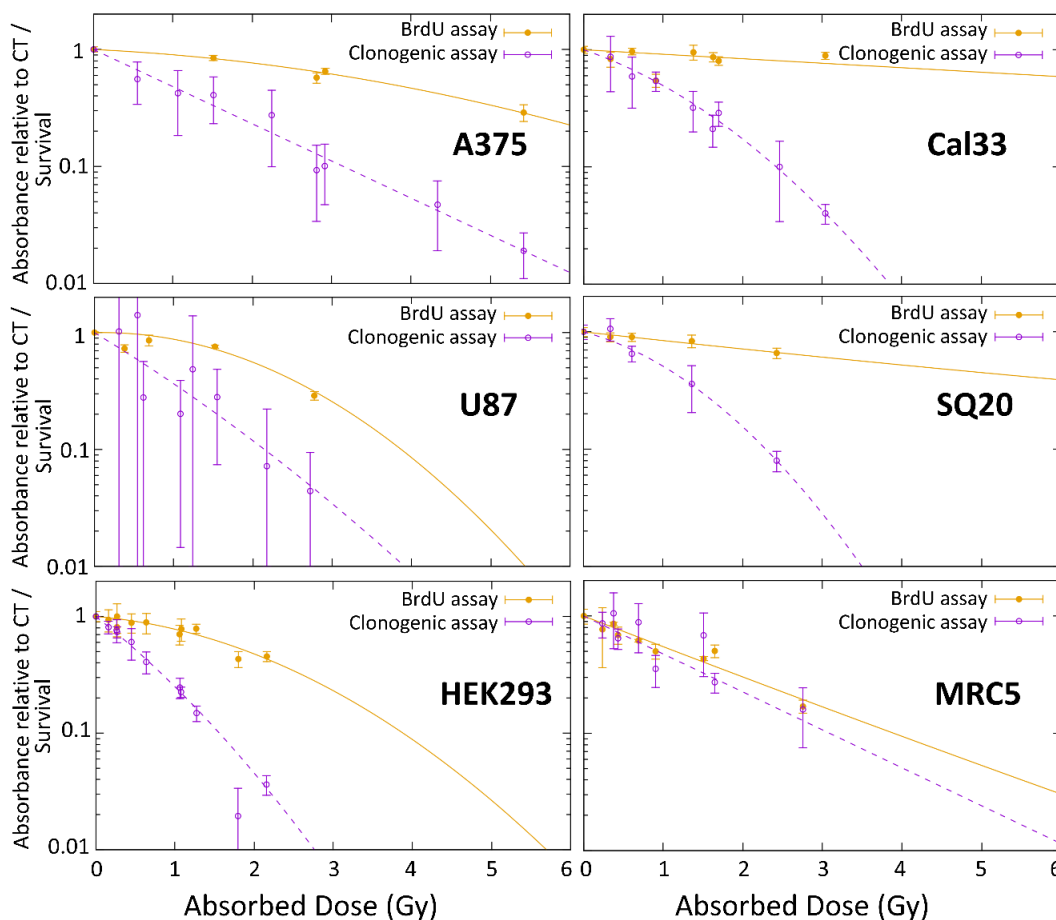


Figure 5. Proliferation and survival data for the different cell lines in response to neutron irradiation. Proliferation (expressed as absorbance relative to control (CT) as determined by BrdU assay), and survival (based on clonogenic assays) are represented for each cell line as a function of the total absorbed dose after neutron irradiation at ILL. Data were obtained from between two and four individual experiments with three replicate dishes plated per point per experiment.

Since a correlation between the two different end-points could not be established, probably because of the time after irradiation at which they are measured, the comparison with photon irradiation and the calculation of RBE factors is limited to the most common end-point used, which is the long-term survival by clonogenic assay.

3.3. Cell survival

Survival data after irradiation, S , studied by clonogenic assays, were fitted using the linear quadratic formula [19]:

$$-\ln S = \alpha D + \beta D^2, \quad (1)$$

where D is the total absorbed dose and α and β are the parameters that describe the behavior of the survival. These parameters are constants that depend on the tissue/cell line and end-point.

For irradiations at the medical LINAC the total dose will correspond to that for the photons only, D_γ , while the survival following irradiations at ILL is due to a dose combination of low-energy neutrons and photons, D_{ILL} . Thus, the total absorbed dose at ILL beam corresponds to the sum of neutron and gamma dose, $D_{ILL} = D_n + D_\gamma$.

From the two fitted survival data, S_{ILL} and S_γ , the survival that corresponds to the neutron effect alone, S_n , can be calculated as:

$$S_n = \frac{e^{-(\alpha_{ILL}D_{ILL} - \beta_{ILL}D_{ILL}^2)}}{e^{-(\alpha_\gamma D_\gamma - \beta_\gamma D_\gamma^2)}}, \quad (2)$$

This survival describes the effect if the dose is due to low-energy neutrons alone, D_n . The data can be fitted to a quadratic function, but given the characteristics of high-LET radiation, the parameter β is assumed to be zero.

Figure 6 shows the survival after neutrons irradiations at ILL (S_{ILL}) and the survival after photon irradiations at HVN medical LINAC (S_γ). As a result of the neutron-induced gamma production in the experimental arrangement, the survival (S_n) associated with the neutron dose alone was obtained by the deduction of the gamma effect, as indicated in eq. (2). The alpha and beta parameters for each one are shown in Table 2.

The U87 cell line was not photon irradiated and results from Bayart *et al.* [20], obtained with a Varian NDI 226 X-ray tube of 200 kVp (kilovolt peak) at a dose rate of 1.2 Gy/min, were used. Also the SQ20 cell line was not irradiated at the medical LINAC; data from Cal33, also squamous cell carcinoma, were used for reference.

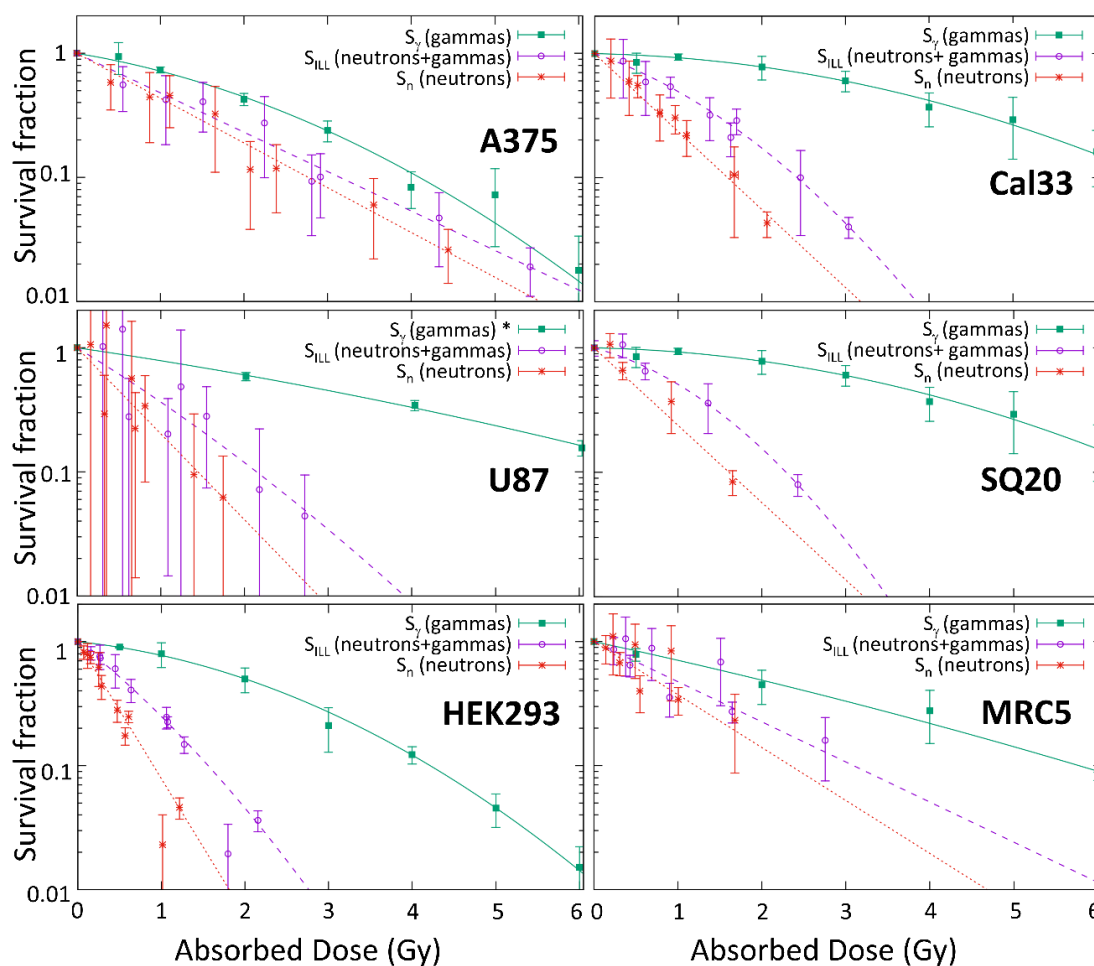


Figure 6. Clonogenic survival of six cell lines as a function of the absorbed dose (Gy) following irradiation with photons at the medical linear accelerator, S_γ , with neutrons at the ILL beam, S_{ILL} , and, derived, ILL neutrons alone, S_n . S_γ for U87 from [20] and S_γ for SQ20 from the one obtained for Cal33. Data were obtained from between two and seven individual experiments after photon irradiation and neutron irradiation. Cells were seeded in triplicate for each data point in each experiment.

Table 2. Alpha and beta values (\pm standard error) for medical linear accelerator irradiations and for the different dose components at ILL.

Cell line	ILL, total		Medical LINAC, photons		ILL, pure neutrons
	α_{ILL} (Gy ⁻¹)	β_{ILL} (Gy ⁻²)	α_{γ} (Gy ⁻¹)	β_{γ} (Gy ⁻¹)	α_n (Gy ⁻¹)
A375	0.73 \pm 0.09	0.00 \pm 0.10	0.25 \pm 0.03	0.070 \pm 0.010	0.83 \pm 0.03
Cal33	0.53 \pm 0.08	0.17 \pm 0.03	0.03 \pm 0.02	0.047 \pm 0.007	1.45 \pm 0.05
U87	0.95 \pm 0.40	0.06 \pm 0.20	0.26 \pm 0.02	0.005 \pm 0.003	1.60 \pm 0.18
SQ20	0.40 \pm 0.20	0.30 \pm 0.10	0.03 \pm 0.02	0.047 \pm 0.007	1.43 \pm 0.12
HEK293	1.20 \pm 0.10	0.16 \pm 0.07	0.16 \pm 0.01	0.091 \pm 0.002	2.54 \pm 0.10
MRC5	0.70 \pm 0.20	0.00 \pm 0.10	0.34 \pm 0.08	0.011 \pm 0.015	0.98 \pm 0.13

3.4. Relative Biological Effectiveness

As mentioned previously, the RBE factors corresponding to thermal neutrons arise mainly from the neutron induced proton emission from nitrogen, $^{14}\text{N}(n,p)^{14}\text{C}$, where the emitted charged particles (protons and ^{14}C) damage the tissue. The RBE of thermal neutrons are calculated from a reference irradiation dose, $D_{\gamma,ref}$, and the dose corresponding to only neutrons, D_n , described by α_n and β_n :

$$RBE_t \text{ or } w_t = \frac{D_{\gamma,ref}}{D_n} \quad (3)$$

The irradiations at the medical LINAC serve as reference irradiation, described with the α_{γ} and β_{γ} previously calculated. For different survival, the corresponding doses calculated with parameters in Table 2, lead to thermal RBE factors shown in Table 3. Data outside the measured range are estimated by extrapolating the curves with the fitting parameters. It is evident that the uncertainty propagation of the cell survival after neutron and photon irradiation leads to huge uncertainties for the deduced RBE values for the cell line MRC5 and large uncertainties for the U87 cell line. Additional experiments with photons and with neutrons are foreseen to reduce this uncertainty and provide meaningful RBE values.

Table 3. Thermal neutron RBE values (w_t factor) for the different cell lines irradiated at ILL as a function of the cell survival fraction.

Survival	A375	Cal33	U87	SQ20	HEK293	MRC5
50%	2.1 \pm 0.3	7.4 \pm 1.1	5.9 \pm 2.7	7.3 \pm 1.5	7.4 \pm 0.2	2.7 \pm 2.7
37%	1.9 \pm 0.3	6.3 \pm 1.0	5.8 \pm 3.0	6.2 \pm 1.3	6.5 \pm 0.2	2.7 \pm 3.1
10%	1.5 \pm 0.3	4.2 \pm 0.7	5.4 \pm 3.2	4.2 \pm 0.9	4.7 \pm 0.1	2.4 \pm 3.3
1%	1.1 \pm 0.2	3.0 \pm 0.5	4.9 \pm 3.1	3.0 \pm 0.7	3.5 \pm 0.1	2.2 \pm 3.1

A new formalism for biological dose estimation has been proposed [7]. It avoids the use of variable RBE factors, and can be considered a simplification of the photon iso-effective dose model [6]. This model makes use of constant weighting factors, shown in Table 4, that do not depend on the survival (or dose), defined as:

$$W_t = \frac{\alpha_n}{\alpha_{\gamma}} \quad (4)$$

Table 4. Constant weighting factors, W_t , of the simplified iso-effective formalism [7].

	A375	Cal33	U87	SQ20	HEK293	MRC5
W_t	3.3 \pm 0.4	48 \pm 32	6.2 \pm 0.8	48 \pm 32	15.9 \pm 1.2	2.9 \pm 0.8

Again, the high errors on the fitting parameters of the irradiations in some of the cell lines lead to high uncertainties, which can be reduced with more irradiation experiments.

4. Discussion

Data showing the biological response of low-energy neutron irradiation shows marked variability for the six cell lines studied. It is therefore crucial to characterize and understand the weighting factors for specific tissues and to avoid having to assume such values.

The proliferation and survival curves obtained following neutron irradiation seem to be different in most cell lines. Although this fact could suggest contradictory results depending on the end-point selected, the proliferative ability of the viable cells was assessed four days after irradiation while the clonogenic assay estimated the long-term cell survival. Moreover, proliferative and clonogenic potential do not have to necessarily correlate as different factors may influence attachment, proliferation and growth, such as cell density and cell-cell contact. Overall, our results suggest that it should be interesting to analyze different parameters as they could provide more information about the possible behavior and response of cells to irradiation *in vivo*.

We have also shown how differences in the nitrogen content between different cell lines have a strong impact on the dose received, emphasizing the importance of the accurate estimation of the elemental composition of each tissue under the neutron field for a better BNCT treatment planning. As we have demonstrated by determining the nitrogen content of HEK293, the CHNS elemental analyzer seems to provide a simple and useful method to measure it.

Survival data suggest that Cal33 and SQ20, which are representative of a similar cancer type, behave in a similar way. They are the most affected after neutron irradiation (compared to photons) and the data were markedly different from the other cell lines. This conclusion must be noted with caution since the nitrogen content of head and neck cancer cells have yet to be confirmed.

Results of the A375 study suggest that this cell line appears to be more radio-resistant to neutrons than the others. The numerical values from previous work [10] are updated, accounting for the specific nitrogen content of this cell line.

The accuracy of the photon irradiation data is also important when used as a reference radiation in the comparison with neutrons for the RBE estimation. A common type of reference photon radiation, at a specific dose rate, would be desirable. Irradiations at the medical linear accelerator at dose rates of few Gy/min are a good option in acquiring data for the reference photon dose, providing a comparison with a standard irradiation field for which there is a lot of clinical experience.

A very important contribution to the especially large uncertainties for the MRC5 cell line is due to the uncertainty of the β value, which makes this value compatible to zero, as it can be seen in Table 2. Although this value is obtained from a more limited set of experiments than the other cell lines, it seems that this cell line is not very representative as a model of the biological response of normal tissues, which are characterized with low α/β ratios for photon irradiation.

It has been shown how with an appropriate experimental arrangement and a clean cold neutron beam, such as the one at ILL, the radiobiological coefficients α_n for thermal neutrons can be obtained with higher precision than has been described previously. Here they have been obtained with an uncertainty of less than 15% for all tumor and normal cell lines.

The data obtained provides very interesting information on the cell types that may be more radio-sensitive to neutron irradiation, and the difference between the tissues. This could be of relevance for BNCT treatment planning when healthy tissues with different neutron sensitivity need to be considered. It would be interesting to study other non-tumor cells of different origins.

Further research work of this type on other cell lines, and *in vivo* studies is desirable to improve the understanding of the biological response to neutrons and for the improvement for BNCT treatment planning.

Supplementary Materials: Supplementary data to this article can be found online at <https://doi.ill.fr/10.5291/ILL-DATA.3-07-376>.

Author Contributions: Conceptualization, M.P., I.P., C.R., M.J.R., U.K. and J.P.; methodology, M.P., I.P., J.P., M.P.S., U.K., T.S., M.H., J.C.R., C.J., D.J., J.L.O., P.A., C.R., M.J.R.; software, M.P., I.P., J.P., J.C.R., C.J., D.J., J.L.O.; validation, C.R., M.J.R.; formal analysis, M.P., I.P., U.K., P.A., C.R., M.J.R.; investigation, M.P., I.P., J.P., U.K., C.R., M.J.R.; resources, I.P., U.K., T.F., C.R.; data curation, M.P., M.J.R.; writing—original draft preparation, M.P., I.P.; writing—review and editing, J.P., M.P.S., U.K., M.H., T.F., J.C.R., C.J., D.J., J.L.O., P.A., C.R., M.J.R.; visualization, M.P., M.J.R.; supervision, I.P., J.P., C.R., U.K., T.F., M.J.R.; project administration, I.P., U.K., T.F., C.R.; funding acquisition, I.P., U.K., T.F. All authors have read and agreed to the published version of the manuscript.

Funding: We acknowledge financial support for this work from the Asociación Española Contra el Cáncer (AECC), project PS16163811PORR (with donations from Bridgestone-FirstStop Spain), the Spanish MINECO under contract FIS2015-69941-C2-1-P, Junta de Andalucía (regional government) under contract P11-FQM-8229, the Campus of International Excellence BioTic (P-BS-64) and the donors of the University of Granada Chair Neutrons for Medicine: the Spanish Fundación ACS, Asociación Capitán Antonio and La Kuadrilla de Iznalloz.

Acknowledgments: We acknowledge Lucie Sancey from the Institute for Advanced Biosciences of Grenoble for kindly share the cell lines and the materials at the Level 2 laboratory at ILL.

Conflicts of Interest: The authors declare no conflict of interest.

References

1. Barth, R.F. *et al.* Current status of boron neutron capture therapy of high grade gliomas and recurrent head and neck cancer. *Radiat. Oncol.* **2012**, *7*, 146–166.
2. Kreiner, A.J. *et al.* Present status of accelerator-based BNCT. *Pract. Oncol. Radiother.* **2016**, *21*, 95–101.
3. Sakurai, Y. Progress In Reactor And Accelerator Based BNCT At Kyoto University Research Reactor Institute, *Proc. of Science* **2017**, 281. DOI: <https://doi.org/10.22323/1.281.0127>
4. Joensuu, H. *et al.* Boron neutron capture therapy of brain tumors: clinical trials at the Finnish facility using boronophenylalanine. *J. Neuro. Oncol.* **2003**, *62*, 123–134.
5. International Atomic Energy Agency. Current Status of Neutron Capture Therapy. *IAEA-TECDOC-1223* **2001**.
6. González, S.J.; Santa Cruz, G.A. The photon-iso-effective dose in boron neutron capture therapy. *Radiat. Res.* **2012**, *178*, 609–621.
7. Pedrosa-Rivera, M.; Praena, J.; Porras, I.; Ruiz-Magaña, M. J.; Ruiz-Ruiz, C. A simple approximation for the evaluation of the photon iso-effective dose in Boron Neutron Capture Therapy based on dose-independent weighting factors. *Appl. Radiat. Isotopes* **2020**, *157*, 109018.
8. Blue, T.E.; Gupta N.; Wollard, J.E. A calculation of the energy dependence of the RBE of neutrons. *Phys. Med. Biol.* **1993**, *38*, 1693-1993.
9. Abele, H. *et al.* Characterization of a ballistic supermirror neutron guide. *Nucl. Instrum. Meth. A* **2006**, *562*, 407-417.
10. Pedrosa-Rivera, M. *et al.* Neutron radiobiology studies with a pure cold neutron beam. *Nucl. Instrum. Meth. B* **2020**, *462*, 24-31.
11. Auterinen, I.; Serén, T.; Anttila, K.; Kosunen, A.; Savolainen, S. Measurement of free beam neutron spectra at eight BNCT facilities worldwide. *Appl. Radiat. Isotopes* **2004**, *61*, 1021-1026.
12. Narayanasamy, G.; Saenz, D.; Cruz, W.; Ha, C. S.; Papanikolaou, N.; Stathakis, S. Commissioning an Elekta Versa HD linear accelerator. *J. App. Clin. Med. Phys.* **2016**, *17*, 179-191.
13. Briesmeister, J. F. X-5 Monte Carlo Team: MCNP—A General Monte Carlo N-Particle Transport Code. **2003**
14. Bedford, J. L.; Childs, P. J.; Nordmark Hansen, V.; Mosleh-Shirazi, M. A.; Verhaegen, F.; Warrington, A. P. Commissioning and quality assurance of the Pinnacle3 radiotherapy treatment planning system for external beam photons. *Br. J. Radiol.* **2003**, *76*, 163-176.
15. Site “Nghia Ho”, URL: https://ngghiaho.com/?page_id=1011 (accessed on 14/04/2020)
16. White, D. R.; Griffith, R. V.; Wilson, I. J. Report 46, Journal of the International Commission on Radiation Units and Measurements **1992**, *24*.
17. Goorley, J. T.; Kiger Iii, W. S.; Zamenhof, R. G. Reference dosimetry calculations for neutron capture therapy with comparison of analytical and voxel models. *Med. Phys.* **2002**, *29*, 145-156.

18. Maughan, R. L.; Chuba, P. J.; Porter, A. T.; Ben-Josef, E.; Lucas, D. R. The elemental composition of tumors: Kerma data for neutrons. *Med. Phys.* **1997**, *24*, 1241-1244.
19. Fowler, J. F. How worthwhile are short schedules in radiotherapy?: A series of exploratory calculations. *Radiat. Oncol.* **1990**, *18*, 165-181.
20. Bayart, E. *et al.* Fast dose fractionation using ultra-short laser accelerated proton pulses can increase cancer cell mortality, which relies on functional PARP1 protein. *Sci. Rep.* **2019**, *9*, 1-10.